

Decoupling-Based LPV Observer for Driver Torque Intervention Estimation in Human-Machine Shared Driving Under Uncertain Vehicle Dynamics

Anh-Tu Nguyen*, *Senior Member, IEEE*, Thierry-Marie Guerra, Chouki Sentouh, Jean-Christophe Popieul

Abstract—This paper proposes a method for simultaneous estimation of both the driver torque and the sideslip angle within the context of human-machine shared driving control for autonomous ground vehicles. To this end, the driver torque is considered as an unknown input (UI) and the sideslip angle is an unmeasured state of the vehicle dynamics system. For simultaneous estimation purpose, a decoupling-based technique is leveraged to design an unknown input observer (UIO). The UIO design goal is to decouple the effect of the unknown driver torque while minimizing the influence of the modeling uncertainties, considered as unknown exogenous disturbances, from the lateral tires forces and the steering system. Linear parameter-varying (LPV) framework is used to deal with the time-varying nature of the vehicle longitudinal speed. Based on Lyapunov stability theory, we derive sufficient conditions, expressed in terms of linear matrix inequality (LMI) constraints, for LPV unknown input observer design. The simultaneous vehicle estimation is reformulated as a convex optimization problem, where the modeling uncertainty influence can be minimized via the ℓ_∞ -gain performance. Hardware-in-the-loop (HiL) tests are performed with the SHERPA dynamic simulator and a human driver to show the effectiveness of the proposed UIO-based estimation method, especially within the cooperative driving control framework.

Note to Practitioners—We present a method to jointly estimate the driver torque and the sideslip angle in the context of human-machine shared driving. To this end, we consider the driver torque as an unknown input and treat the sideslip angle as an unmeasured state of the vehicle dynamics system. The core of our method lies in the application of a decoupling-based technique to design an unknown input observer. The primary objective of this UIO is to effectively decouple the influence of the unknown driver torque while mitigating the impact of modeling uncertainties, considered as unknown exogenous disturbances, on the lateral tire forces and the steering system. Using an LPV framework has allowed the time-varying nature of the vehicle longitudinal velocity to be effectively addressed. Via Lyapunov stability theory, we have established sufficient conditions, expressed in terms of LMI constraints, for the design of the LPV unknown input observer. The proposed simultaneous vehicle estimation method has been reformulated as a convex optimization problem, allowing to minimize the influence of modeling uncertainties. To show the effectiveness of the proposed

UIO-based estimation method, we have conducted extensive HiL tests using the SHERPA dynamic simulator with a human driver. The real-time experiments demonstrate the effectiveness of the proposed method, especially with respect to related estimation results in the literature, within the cooperative driving control framework. The proposed LPV estimation method contributes to the advancement of the field of autonomous ground vehicles by providing practitioners with a robust tool for joint estimation of essential variables critical for effective vehicle control and safety in the context of human-machine cooperative driving.

Index Terms—Driver steering intervention, driver torque estimation, driver-automation shared driving, sideslip angle, unknown input observer, LPV technique.

I. INTRODUCTION

The real-time information of the vehicle dynamics and the driver steering intervention are crucial to develop advanced driver assistance systems (ADAS) for intelligent vehicles (IVs), *e.g.*, online driver monitoring systems [1]–[3], active safety control systems [4]–[6], shared driving control systems [7]–[9]. However, commercial onboard vehicle sensors used to measure the vehicle dynamics and to monitor the driver's actions are generally expensive, which may not be available for commercial vehicle applications [10], [11]. Especially, in several situations, the human driver variables cannot be even obtained by physical sensors [12], [13]. Therefore, estimating the vehicle dynamics as well as the driver's actions, *e.g.*, driver steering torque, has received great attention over the past decade [1], [3], [14].

Within the human-machine shared driving control framework of IVs, the driver has the option to assume control of the vehicle when experiencing uncertainty or doubt. Hence, the detection of the driver intervention plays a critical role in performing driving tasks [15]. Moreover, understanding the driver-automation interaction necessitates precise knowledge of driver steering interventions [16]. This knowledge is essential to effectively balance the control authority between humans and machines, thereby enabling seamless assistance to human drivers across diverse driving conditions [7], [8], [17]. Recent research has provided evidence that the detection of driver interventions is feasible [18]–[21]. However, the primary limitations of existing approaches encompass the requirement of supplementary hardware, the substantial CPU load for data processing, the associated costs, etc. [15], [22]. Furthermore, accurately measuring the driver steering torque using physical sensors is challenging due to the intricate

This research is sponsored by the RITMEA project, the Hauts-de-France Region, the European Community, the Regional Delegation for Research and Technology, the Ministry of Higher Education and Research, and the French National Center for Scientific Research (CNRS). This work has been done within the framework of the CoCoVeIA project (ANR-19-CE22-0009-01) and the HM-Science project (ANR-21-CE48-0021), funded by the Agence Nationale de la Recherche.

The authors are with the LAMIH laboratory, UMR CNRS 8201, Université Polytechnique Hauts-de-France, Valenciennes, France. A.-T. Nguyen, C. Sentouh and J.-C. Popieul are also with the INSA Hauts-de-France, Valenciennes, France. *Corresponding author (e-mail: nguyen.trananhthu@gmail.com).

coupling between driver torque, assistance torque, and unknown friction torque inherent in the steering process [12], [23]. To overcome this challenge, model-based estimation approaches emerge as promising solutions. Remarkably, the current literature lacks comprehensive exploration and investigation into model-based estimation methods for driver steering interventions [1], [21].

The authors in [15] presented and tested a driver intervention detection algorithm by estimating the steering system dynamics. However, this transfer-function-based method cannot provide a real-time information about the driver's steering torque. Based on the steering wheel actuation dynamics, a nonlinear disturbance observer was proposed in [12] to estimate the driver steering torque in a steer-by-wire system. However, the torque estimation results may exhibit high sensitivity to parametric uncertainties and disturbances. Consequently, substantial efforts are still needed for a comprehensive theoretical analysis of the accuracy and robustness of this observer design method concerning uncertainties and noises. An $\mathcal{H}_\infty/\mathcal{H}_2$ proportional multi-integral (PMI) observer was used in [24] to estimate the driver torque from the dynamics of an electric power steering (EPS) system. Based on a linear uncertain model of a steer-by-wire system, an \mathcal{H}_2 observer was synthesized in [14] for driver torque estimation. Note that the vehicle dynamics, essential for active safety control design, cannot be estimated with the methods in [12], [14], [24]. Soualmi et al. [25] proposed an PMI observer for a simultaneous estimation of vehicle dynamics and driver steering torque. As in [14], the \mathcal{D} -stability concept was also taken into account in the observer design to improve the estimation performance. However, the design of PMI observers in [14], [24], [25] assume that the unknown driver torque signal is piecewise constant, which is not always compatible with IVs applications, especially when considering unexpected driving maneuvers. To avoid this issue, a linear parameter-varying (LPV) estimation method was proposed in [21] to jointly estimate the vehicle dynamics and the driver torque without requiring any *a priori* torque information. However, in [21] the driver steering torque was considered as an unknown disturbance, which has a direct and persistent impact on the estimation error dynamics. Therefore, the estimation quality may be degraded when the variation of the driver torque becomes large. Moreover, a Taylor's approximation was used to reduce the complexity and conservatism of the LPV observer design, which further yields modeling errors. The fuzzy UIO introduced in [10] can address this drawback. However, implementing this method in real-time may pose practical challenges due to a significant number of subsystems required for fuzzy representation and a conservative Lipschitz-like assumption, as discussed in [26]. Moreover, this UIO only allows to estimate the steering angle control of autonomous vehicles, not directly the driver steering torque.

Motivated by the aforementioned concerns, this paper investigates the simultaneous estimation of driver steering torque and vehicle dynamics in the context of human-machine shared driving control. To this end, a polytopic LPV modeling method is used to represent the driver-vehicle system dynamics while taking into account the time-varying nature of the vehicle

speed parameter. The modeling uncertainties, issued from the lateral tires forces and the steering system, are considered as unknown exogenous disturbances. In particular, an UI decoupling technique is leveraged to cancel the effect of the unknown driver torque on the vehicle state estimation error dynamics. Considering the class of amplitude-bounded disturbances, practically encountered in driver-vehicle system applications, their influence is minimized via an ℓ_∞ -gain performance, *i.e.*, peak-to-peak disturbance attenuation. An asymptotic convergence of both vehicle dynamics and driver torque estimation errors can be theoretically achieved when the disturbances vanish, which is not the case in [21]. Note also that the modeling uncertainties, specifically related to the lateral tires forces and the EPS dynamics, have not been taken into account in the LPV observer design in [21]. Using Lyapunov stability theory, sufficient conditions are derived for the parameter-dependent UIO design. The design conditions are expressed in terms of linear matrix inequalities (LMIs), which can be effectively solved using semidefinite programming techniques [27]. Specifically, the contributions of the paper can be summarized as follows.

- An UIO-based estimation method to jointly estimate the sideslip angle and the driver steering intervention for human-machine shared driving, which is not the case of [12], [14], [24]. Compared to the LPV estimation method in [21], asymptotic convergence of the estimation error can be achieved for a nominal vehicle system.
- The proposed LPV observer design does not rely on assumptions about the driver torque, unlike previous works [14], [24], [25], or LPV model approximation [21]. Instead, it considers modeling uncertainties of tire forces and EPS dynamics to enhance estimation performance.
- The robust estimation performance is theoretically ensured using Lyapunov stability theory. The UIO design is recast as a convex optimization problem under LMI constraints, easily solvable using standard numerical solvers.
- Hardware-in-the-loop (HiL) tests are performed with the SHERPA driving simulator and a human driver to validate the effectiveness of the proposed UIO-based estimation method. Furthermore, we compare the new method with the LPV observer from [21], known for superior estimation performance over the PMI observer from [25], highlighting the practical significance of our approach.

Notation. \mathbb{N} is the set of non-negative integers, and we denote $\mathcal{I}_p = \{1, 2, \dots, p\} \subset \mathbb{N}$. For a matrix X , X^\top denotes its transpose, $X \succ 0$ means that X is positive definite, $\text{He}X = X + X^\top$, and X^\dagger denotes its Moore–Penrose pseudo-inverse. For a vector $\mathbf{x} \in \mathbb{R}^n$, we denote its 2-norm as $\|\mathbf{x}\| = \sqrt{\mathbf{x}^\top \mathbf{x}}$. For a sequence of vectors $\{\mathbf{x}_k\}_{k \in \mathbb{N}}$, we denote $\|\mathbf{x}\|_{\ell_\infty} = \sup_{k \geq 0} \|\mathbf{x}_k\|$. Then, $\{\mathbf{x}_k\}_{k \in \mathbb{N}} \in \ell_\infty$ if $\|\mathbf{x}\|_{\ell_\infty} < \infty$. $\text{diag}\{X_1, X_2\}$ denotes a block-diagonal matrix composed of X_1 and X_2 . I is the identity matrix of appropriate dimension. The symbol “ \star ” stands for the terms deduced by symmetry.

II. VEHICLE MODELING AND PROBLEM DEFINITION

This section reviews the main features of the vehicle dynamics. Then, the related UIO design problem is formulated. The vehicle parameters are given in Table I.

TABLE I
VEHICLE PARAMETERS.

Parameter	Symbol	Value
Distance from the CoG to front axle	l_f	1.3 [m]
Distance from the CoG to rear axle	l_r	1.6 [m]
Tire length contact	η_t	0.13 [m]
Steering gear ratio	R_s	16 [-]
Steering system damping	B_s	5.73 [-]
Manual steering column coefficient	K_p	0.5 [-]
Vehicle mass	M_v	2052 [kg]
Inertia of vehicle yaw moment	I_z	2800 [kgm ²]
Inertia of steering system	I_s	0.05 [kgm ²]
Front cornering stiffness	C_f	57000 [N/rad]
Rear cornering stiffness	C_r	59000 [N/rad]

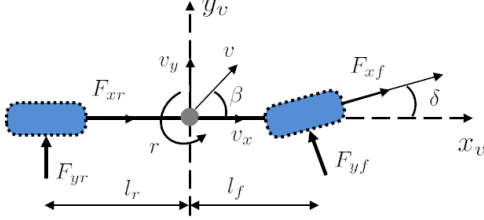


Fig. 1. Schematic of a 2-DOF vehicle model.

A. Nonlinear Vehicle Dynamics

A nonlinear single track model is used to represent the vehicle motion in the horizontal plane, see Fig. 1. This model captures the essential vehicle dynamics, described as [28]

$$\begin{aligned} M_v(\dot{v}_x - rv_y) &= F_{xf} \cos \delta - F_{yf} \sin \delta + F_{xr} \\ M_v(\dot{v}_y + rv_x) &= F_{xf} \sin \delta + F_{yf} \cos \delta + F_{yr} \\ I_z \dot{r} &= l_f(F_{xf} \sin \delta + F_{yf} \cos \delta) - l_r F_{yr} \end{aligned} \quad (1)$$

where v_x is the vehicle longitudinal speed, v_y is the vehicle lateral speed, r is the vehicle yaw rate, δ is the front wheel steering angle. The cornering longitudinal/lateral forces at the front/rear tires are denoted by F_{pq} , with $p \in \{x, y\}$ and $q \in \{f, r\}$. Using the Pacejka magic formula [29], the front/rear lateral forces can be modeled as

$$F_{yq}(\alpha_q) = \mathcal{D}_q \sin(\nabla_q), \quad q \in \{f, r\} \quad (2)$$

with $\nabla_q = C_q \text{atan}[(1 - \mathcal{E}_q) \mathcal{H}_q \alpha_q + \mathcal{E}_q \text{atan}(\mathcal{H}_q \alpha_q)]$. The corresponding Pacejka parameters \mathcal{H}_q , C_q , \mathcal{D}_q and \mathcal{E}_q depend on the characteristics of the tires, the roads and the vehicle operating conditions. The sideslip angles for the front and rear tires can be modeled as

$$\alpha_f = \delta - \text{atan}\left(\frac{v_y + l_f r}{v_x}\right), \quad \alpha_r = \text{atan}\left(\frac{l_r r - v_y}{v_x}\right). \quad (3)$$

The EPS dynamics can be described as [30]

$$I_s R_s \ddot{\delta} + R_s B_s \dot{\delta} = T_s - T_{al} + T_w \quad (4)$$

where the total steering torque $T_s = T_a + T_d$ is composed of the assistance torque T_a and the driver torque T_d . The uncertain torque T_w represents the EPS uncertainty, specifically related to the self-aligning torque T_{al} , which is modeled as

$$T_{al} = \frac{2K_s C_f \eta_t}{R_s} \left(\delta - \frac{v_y + l_f r}{v_x} \right).$$

B. Estimation Problem Statement

Despite its crucial importance to active safety control systems, the real-time information of the sideslip angle β and the driver torque T_d cannot be always reliably obtained from onboard sensors. In particular, with a human-machine shared control perspective, we assume that the driver's driving action T_d can be "unpredictable" and needs to be reconstructed. This paper provides a cost-effective solution to reconstruct such information via an UIO with the following requirements.

- The new UIO structure can be easily designed and implemented with only measurements from low-cost sensors.
- The estimation errors of both the sideslip angle and the driver steering torque are norm-bounded, specified by an ℓ_∞ -gain level, which can be set *arbitrarily* small via a convex optimization problem.
- The estimation robustness with respect to the time-varying speed and the vehicle dynamics uncertainties can be guaranteed with Lyapunov stability theory.

Note that the sideslip angle β can be expressed by $\beta = \text{atan}\left(\frac{v_y}{v_x}\right)$ [29]. Then, the estimation of the lateral speed v_y is considered as equivalent to the estimation of the sideslip angle β . Fig. 2 depicts the proposed UIO scheme, whose design is presented in Section IV.

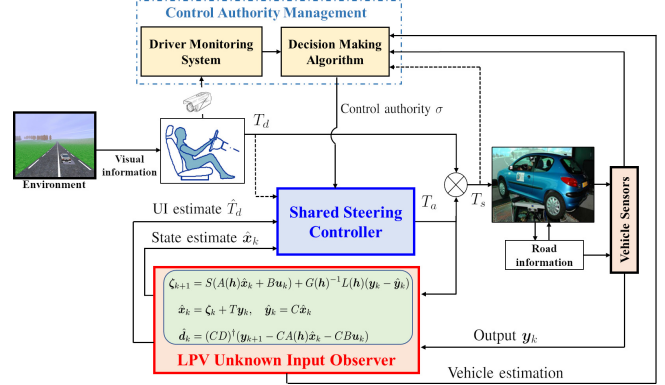


Fig. 2. LPV unknown input observer scheme within the context of human-machine shared driving control.

III. LPV REPRESENTATION OF VEHICLE SYSTEM

We represent hereafter the vehicle system in a polytopic LPV form, which is suitable for UIO design purposes.

A. Observer-Based Uncertain Vehicle System

To derive the observer-based vehicle model, we assume that [28], [29]: (i) the vehicle speed is a time-varying parameter; (ii) the lateral tires forces are proportional to the slip angles of each axle; (iii) the small angle assumption is considered. Note that these assumptions are appropriate for normal driving under mild acceleration conditions. Then, the lateral tires forces in (2) can be linearized as follows [31]:

$$\begin{aligned} F_{yf} &= 2C_f (1 + W_f \Delta(\alpha_f)) \alpha_f \\ F_{yr} &= 2C_r (1 + W_r \Delta(\alpha_r)) \alpha_r \end{aligned} \quad (5)$$

where the sideslip angles in (3) become

$$\alpha_f = \delta - \frac{v_y + l_f r}{v_x}, \quad \alpha_r = \frac{l_r r - v_y}{v_x}. \quad (6)$$

The term $\Delta(\alpha_f)$ (respectively $\Delta(\alpha_r)$) represents the nonlinear part of F_{yf} (respectively F_{yr}). Since $\Delta(\alpha_q)$, for $q \in \{f, r\}$, is considered as uncertainties of the lateral tires forces, it can be normalized as $-1 \leq \Delta(\alpha_q) \leq 1$. Moreover, W_q , for $q \in \{f, r\}$, is a weight used for normalization for which $2C_q(1 + W_q)$ and $2C_q(1 - W_q)$, for $q \in \{f, r\}$, are respectively the upper and lower bounds of the slopes of the lateral forces characteristics [31], *i.e.*,

$$2C_q(1 - W_q) \leq \frac{\partial}{\partial \alpha_q} F_{yq} \leq 2C_q(1 + W_q), \quad q \in \{f, r\}.$$

Let us denote $F_f = \Delta(\alpha_f)\alpha_f$ and $F_r = \Delta(\alpha_r)\alpha_r$ as modeling uncertainties related to the lateral tires forces. The uncertain lateral tires forces in (5) can be reformulated as

$$\begin{aligned} F_{yf} &= 2C_f\alpha_f + 2C_fW_fF_f \\ F_{yr} &= 2C_r\alpha_r + 2C_rW_rF_r. \end{aligned} \quad (7)$$

From (1), (4), (6) and (7), the vehicle dynamics can be represented in the following state-space form:

$$\dot{\mathbf{x}} = A_v(v_x)\mathbf{x} + B_v\mathbf{u} + D_v\mathbf{d} + E_v\mathbf{w} \quad (8)$$

where $\mathbf{x} = [v_y \ r \ \delta \ \dot{\delta}]^\top$ is the system state, $\mathbf{u} = T_a$ is the known input, $\mathbf{d} = T_d$ is the unknown input that needs to be estimated, and $\mathbf{w} = [F_f \ F_r \ T_w]^\top$ represents vehicle dynamics uncertainties. The state-space matrices of system (8) are given by

$$\begin{aligned} A_v(v_x) &= \begin{bmatrix} a_{11} & a_{12} & a_{13} & 0 \\ a_{21} & a_{22} & a_{23} & 0 \\ 0 & 0 & 0 & 1 \\ a_{41} & a_{42} & a_{43} & a_{44} \end{bmatrix}, & B_v &= \begin{bmatrix} 0 \\ 0 \\ 0 \\ \frac{1}{I_s R_s} \end{bmatrix} \\ E_v &= \begin{bmatrix} \frac{2C_f W_f}{M_v} & \frac{2C_r W_r}{M_v} & 0 \\ \frac{2C_f W_f l_f}{I_z} & \frac{-2C_r W_r l_r}{I_z} & 0 \\ 0 & 0 & 0 \\ 0 & 0 & \frac{1}{I_s R_s} \end{bmatrix}, & D_v &= \begin{bmatrix} 0 \\ 0 \\ 0 \\ \frac{1}{I_s R_s} \end{bmatrix} \end{aligned}$$

with

$$\begin{aligned} a_{11} &= -\frac{2(C_r + C_f)}{M_v v_x}, & a_{12} &= \frac{2(l_r C_r - l_f C_f)}{M_v v_x} - v_x \\ a_{21} &= \frac{2(l_r C_r - l_f C_f)}{I_z v_x}, & a_{22} &= -\frac{l_r^2 C_r + l_f^2 C_f}{I_z v_x} \\ a_{41} &= \frac{2K_p C_f \eta_t}{I_s R_s^2 v_x}, & a_{42} &= \frac{2K_p C_f l_f \eta_t}{I_s R_s^2 v_x} \\ a_{43} &= -\frac{2K_p C_f \eta_t}{I_s R_s^2}, & a_{44} &= -\frac{B_s}{I_s} \\ a_{13} &= \frac{2C_f}{M_v}, & a_{23} &= \frac{2l_f C_f}{I_z}. \end{aligned}$$

As in practice, we assume that the yaw rate r can be measured by an inertial navigation system. The steering angle δ and steering rate $\dot{\delta}$ can be obtained by an onboard optical encoder. However, the measurement of the lateral speed v_y or the sideslip angle β is unavailable for commercial vehicle

applications due to sensor cost reasons [10], [32]. Hence, the output equation of system (8) is given by

$$\mathbf{y} = C\mathbf{x}, \quad C = \begin{bmatrix} 0 & 1 & 0 & 0 \\ 0 & 0 & 1 & 0 \\ 0 & 0 & 0 & 1 \end{bmatrix}.$$

Using Euler's discretization method, with a sampling time $t_s = 0.01$ [s], the discrete-time counterpart of the vehicle model (8) is given by

$$\begin{aligned} \mathbf{x}_{k+1} &= A(v_x)\mathbf{x}_k + B\mathbf{u}_k + D\mathbf{d}_k + E\mathbf{w}_k \\ \mathbf{y}_k &= C\mathbf{x}_k \end{aligned} \quad (9)$$

with

$$A(v_x) = t_s A_v(v_x) + I, \quad B = t_s B_v, \quad D = t_s D_v, \quad E = t_s E_v.$$

For UIO design, we reformulate in the sequel the vehicle model (9) in a numerically tractable LPV representation.

B. Polytopic LPV Representation of Vehicle System

There are two *dependently* varying parameters involved in the dynamics of the LPV vehicle system (9), *i.e.*, $A(v_x) = A(\boldsymbol{\theta})$, with $\boldsymbol{\theta} = [\theta_1 \ \theta_2]^\top$, $\theta_1 = v_x$ and $\theta_2 = \frac{1}{v_x}$. Note that the vehicle speed is measured and bounded as

$$v_{\min} \leq v_x \leq v_{\max}$$

with $v_{\min} = 5$ [m/s] and $v_{\max} = 30$ [m/s]. These two time-varying parameters form a convex hull \mathcal{P}_θ with four vertices

$$\begin{aligned} \theta_{v1} &= [v_{\min} \ \frac{1}{v_{\min}}]^\top, & \theta_{v2} &= [v_{\min} \ \frac{1}{v_{\max}}]^\top \\ \theta_{v3} &= [v_{\max} \ \frac{1}{v_{\max}}]^\top, & \theta_{v4} &= [v_{\max} \ \frac{1}{v_{\min}}]^\top. \end{aligned}$$

Observe in Fig. 3 that the parameter polytope \mathcal{P}_θ with four vertices leads to design conservatism and numerical complexity. This is due to the fact that v_x and $\frac{1}{v_x}$ are separately considered despite its strong dependency. Note that v_x and $\frac{1}{v_x}$ only evolve on the curve \mathcal{C} , and the vertices θ_{v2} and θ_{v4} are *unreachable* for any value of v_x . To take into account this strong dependency and to reduce the numerical complexity for observer design, a Taylor's approximation-based variable change has been widely adopted to derive an approximated LPV model for system (9) as in [21], [30]. However, such an approximation leads to modeling errors, which can deteriorate the estimation performance. To avoid this issue, here we exactly characterize the parameter space with the three vertices θ_{v1} , θ_{v2} and θ_{v3} . Hence, the vehicle system (9) can be equivalently represented by the following polytopic LPV model:

$$\begin{aligned} \mathbf{x}_{k+1} &= \sum_{i=1}^3 h_i(\boldsymbol{\theta}_k) A_i \mathbf{x}_k + B\mathbf{u}_k + D\mathbf{d}_k + E\mathbf{w}_k \\ \mathbf{y}_k &= C\mathbf{x}_k \end{aligned} \quad (10)$$

where the linear submodels A_i , for $i = \mathcal{I}_3$, are given by

$$\begin{aligned} A_1 &= A(\theta_{1 \min}, \theta_{2 \max}) \\ A_2 &= A(\theta_{1 \min}, \theta_{2 \min}) \\ A_3 &= A(\theta_{1 \max}, \theta_{2 \min}). \end{aligned}$$

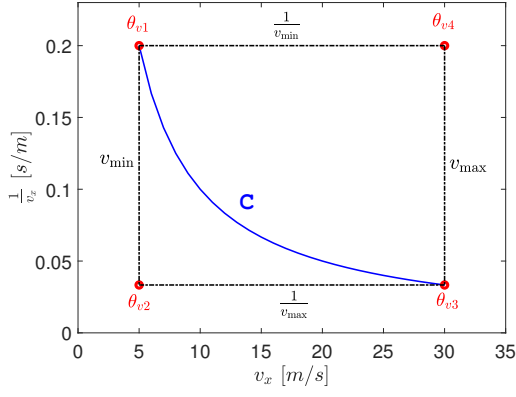


Fig. 3. Four-vertices polytope \mathcal{P}_θ of parameter θ .

The membership functions $h_i(\boldsymbol{\theta}_k)$ in (10), for $i \in \mathcal{I}_3$, are constructed as

$$\begin{bmatrix} \theta_{1 \min} & \theta_{1 \min} & \theta_{1 \max} \\ \theta_{2 \max} & \theta_{2 \min} & \theta_{2 \min} \\ 1 & 1 & 1 \end{bmatrix} \begin{bmatrix} h_1(\boldsymbol{\theta}_k) \\ h_2(\boldsymbol{\theta}_k) \\ h_3(\boldsymbol{\theta}_k) \end{bmatrix} = \begin{bmatrix} \theta_{1k} \\ \theta_{2k} \\ 1 \end{bmatrix}.$$

Note that the membership functions $h_i(\boldsymbol{\theta}_k)$, for $i \in \mathcal{I}_3$, satisfy the following convex sum property:

$$h_i(\boldsymbol{\theta}_k) \geq 0, \quad \sum_{i=1}^3 h_i(\boldsymbol{\theta}_k) = 1.$$

With the LPV polytopic form (10), we propose an UIO-based estimation method for system (9) in the next section.

IV. LPV UNKNOWN INPUT OBSERVER DESIGN

This section first formulates the UIO design problem. Then, we present a method to design an LPV observer with ℓ_∞ -performance guarantee.

A. Problem Formulation

For generality of UIO design, we consider the LPV vehicle model (10) in its more general form

$$\begin{aligned} \mathbf{x}_{k+1} &= A(\mathbf{h})\mathbf{x}_k + B\mathbf{u}_k + D\mathbf{d}_k + E\mathbf{w}_k \\ \mathbf{y}_k &= C\mathbf{x}_k \end{aligned} \quad (11)$$

where $\mathbf{x}_k \in \mathbb{R}^{n_x}$ is the state vector, $\mathbf{y}_k \in \mathbb{R}^{n_y}$ is the output vector, $\mathbf{u}_k \in \mathbb{R}^{n_u}$ is the known input vector, $\mathbf{d}_k \in \mathbb{R}^{n_d}$ is the unknown input vector, and $\mathbf{w}_k \in \mathbb{R}^{n_w}$ is the disturbance vector. The matrix $A(\mathbf{h})$ is given in a polytopic form as

$$A(\mathbf{h}) = \sum_{i=1}^{n_r} h_i(\boldsymbol{\theta}_k) A_i$$

where $\boldsymbol{\theta}_k \in \mathbb{R}^{n_\theta}$ is the vector of scheduling parameters, and the membership functions satisfy the convex sum property

$$\sum_{i=1}^{n_r} h_i(\boldsymbol{\theta}_k) = 1, \quad 0 \leq h_i(\boldsymbol{\theta}_k) \leq 1. \quad (12)$$

Let \mathcal{H} be the set of membership functions satisfying condition (12), and

$$\begin{aligned} \mathbf{h} &= [h_1(\boldsymbol{\theta}_k), h_2(\boldsymbol{\theta}_k), \dots, h_{n_r}(\boldsymbol{\theta}_k)]^\top \in \mathcal{H} \\ \mathbf{h}_+ &= [h_1(\boldsymbol{\theta}_{k+1}), h_2(\boldsymbol{\theta}_{k+1}), \dots, h_{n_r}(\boldsymbol{\theta}_{k+1})]^\top \in \mathcal{H}. \end{aligned}$$

For UIO design, we consider the following assumption for system (11).

Assumption 1. We assume that system (11) verifies the following rank condition:

$$\begin{aligned} \text{rank} \begin{bmatrix} I & D \\ C & 0 \end{bmatrix} &= n_x + n_d \\ \text{rank}(CD) &= \text{rank}(D). \end{aligned} \quad (13)$$

Remark 1. The rank condition (13) is standard for unknown input decoupling in UIO design [10], [11], [33], [34]. Note that the vehicle system (10) verifies these rank conditions.

To jointly estimate the state \mathbf{x}_k and the unknown input \mathbf{d}_k , we consider the following parameter-dependent UIO structure:

$$\begin{aligned} \boldsymbol{\zeta}_{k+1} &= S(A(\mathbf{h})\hat{\mathbf{x}}_k + B\mathbf{u}_k) + G(\mathbf{h})^{-1}L(\mathbf{h})(\mathbf{y}_k - \hat{\mathbf{y}}_k) \\ \hat{\mathbf{x}}_k &= \boldsymbol{\zeta}_k + T\mathbf{y}_k \\ \hat{\mathbf{y}}_k &= C\hat{\mathbf{x}}_k \\ \hat{\mathbf{d}}_k &= (CD)^\dagger(\mathbf{y}_{k+1} - CA(\mathbf{h})\hat{\mathbf{x}}_k - CB\mathbf{u}_k) \end{aligned} \quad (14)$$

with

$$[G(\mathbf{h}) \quad L(\mathbf{h})] = \sum_{i=1}^{n_r} h_i(\boldsymbol{\theta}_k) [G_i \quad L_i]. \quad (15)$$

The matrices S , T , $G(\mathbf{h})$ and $L(\mathbf{h})$ of the LPV observer (14) are to be designed such that the following UI decoupling constraints are verified:

$$S + TC = I, \quad SD = 0. \quad (16)$$

Remark 2. Selecting $S = I$ and $T = 0$, the unknown input observer (14) is reduced to the well-known Luenberger observer structure, largely employed in the literature [14], [21], [25]. Then, with a more general structure than the classical Luenberger observer, the proposed UIO allows for a joint estimation of the sideslip angle and the driver steering torque. Note also that the matrices S and T cannot be parameter-dependent due to the algebraic compatibility required by the decoupling constraints in (16).

Define the estimation error as $\mathbf{e}_k = \mathbf{x}_k - \hat{\mathbf{x}}_k$. Then, the dynamics of \mathbf{e}_k can be derived from (11) and (14) as

$$\begin{aligned} \mathbf{e}_{k+1} &= \mathbf{x}_{k+1} - \hat{\mathbf{x}}_{k+1} \\ &= (S + TC)\mathbf{x}_{k+1} - \hat{\mathbf{x}}_{k+1} \\ &= S\mathbf{x}_{k+1} + T\mathbf{y}_{k+1} - (\boldsymbol{\zeta}_{k+1} + T\mathbf{y}_{k+1}) \\ &= S(A(\mathbf{h})\mathbf{e}_k + D\mathbf{d}_k + E\mathbf{w}_k) - G(\mathbf{h})^{-1}L(\mathbf{h})(\mathbf{y}_k - \hat{\mathbf{y}}_k). \end{aligned} \quad (17)$$

Taking into account the constraint $SD = 0$ in (16), the estimation error dynamics (17) can be rewritten as

$$\mathbf{e}_{k+1} = \mathcal{A}(\mathbf{h})\mathbf{e}_k + SE\mathbf{w}_k \quad (18)$$

with $\mathcal{A}(\mathbf{h}) = SA(\mathbf{h}) - G(\mathbf{h})^{-1}L(\mathbf{h})C$. Moreover, it follows from (11) that

$$\mathbf{d}_k = (CD)^\dagger(\mathbf{y}_{k+1} - CA(\mathbf{h})\mathbf{x}_k - CB\mathbf{u}_k - CE\mathbf{w}_k). \quad (19)$$

We define the UI estimation error as $\boldsymbol{\varepsilon}_k = \hat{\mathbf{d}}_k - \mathbf{d}_k$. From (14) and (19), we have

$$\boldsymbol{\varepsilon}_k = (CD)^\dagger(CA(\mathbf{h})\mathbf{e}_k + CE\mathbf{w}_k).$$

For estimation purposes, we introduce the performance output \mathbf{z}_k associated to system (18) as the vector of estimation errors

$$\mathbf{z}_k = \begin{bmatrix} \mathbf{e}_k \\ \boldsymbol{\varepsilon}_k \end{bmatrix} = \mathcal{C}(\mathbf{h}) \begin{bmatrix} \mathbf{e}_k \\ \mathbf{w}_k \end{bmatrix} \quad (20)$$

with

$$\mathcal{C}(\mathbf{h}) = \begin{bmatrix} I & 0 \\ (CD)^\dagger CA(\mathbf{h}) & (CD)^\dagger CE \end{bmatrix}. \quad (21)$$

We are ready to formulate the following UIO design problem.

Problem 1. Consider the LPV system (11) with the unknown input observer (14). Determine the matrices S , T , $G(\mathbf{h})$ and $L(\mathbf{h})$ such that the estimation error dynamics (18) verifies the following closed-loop properties.

- (P1) If $\mathbf{w}_k = 0$, for $\forall k \in \mathbb{N}$, the error dynamics (18) is exponentially stable with a decay rate $\alpha \in (0, 1)$.
- (P2) The error \mathbf{e}_k is uniformly bounded for any initial condition \mathbf{e}_0 and any sequence $\{\mathbf{w}_k\}_{k \in \mathbb{N}} \in \ell_\infty$. That is, there exists a bound $\varphi(\mathbf{e}_0, \|\mathbf{w}\|_{\ell_\infty})$ such that $\|\mathbf{e}_k\| \leq \varphi(\mathbf{e}_0, \|\mathbf{w}\|_{\ell_\infty})$, for $\forall k \geq 0$. Moreover, the performance output verifies

$$\limsup_{k \rightarrow \infty} \|\mathbf{z}_k\| < \gamma \|\mathbf{w}\|_{\ell_\infty} \quad (22)$$

where the ℓ_∞ -gain γ is specified in Theorem 1. We also deduce from (22) that if $\mathbf{e}_0 = 0$, then $\|\mathbf{z}_k\| < \gamma \|\mathbf{w}\|_{\ell_\infty}$, for $\forall k \in \mathbb{N}$.

Remark 3. System (18) verifying properties (P1)–(P2) is said to be globally uniformly ℓ_∞ -stable with a performance level γ , see [35, Chapter 4]. It follows from (20) and (22) that a smaller value of the ℓ_∞ -gain γ leads to a better estimation performance. Note also that a larger value of the decay rate α yields faster error convergence, possibly causing aggressive estimation behaviors.

Remark 4. For the vehicle system (9), since \mathbf{w}_k represents the modeling uncertainties stemmed from the lateral tires forces in (7) and the EPS dynamics in (4), then it is always physically bounded in amplitude, i.e., $\{\mathbf{w}_k\}_{k \in \mathbb{N}} \in \ell_\infty$. Here, the ultimate amplitude bound $\|\mathbf{w}\|_{\ell_\infty}$ is not required for UIO design.

The following technical lemmas are useful for UIO design.

Lemma 1 ([36]). Consider the parameter-dependent inequality

$$\Upsilon_{hh_+} = \sum_{i=1}^{n_r} \sum_{j=1}^{n_r} \sum_{l=1}^{n_r} h_i(\boldsymbol{\theta}_k) h_j(\boldsymbol{\theta}_k) h_l(\boldsymbol{\theta}_{k+1}) \Upsilon_{ijl} \prec 0 \quad (23)$$

where $\mathbf{h}, \mathbf{h}_+ \in \mathcal{H}$. The symmetric matrices of appropriate dimensions Υ_{ijl} , with $i, j, l \in \mathcal{I}_{n_r}$, are linearly dependent on the unknown decision variables. Then the parameter-dependent inequality (23) holds if

$$\begin{aligned} \Upsilon_{iil} &\prec 0, \quad i, l \in \mathcal{I}_{n_r} \\ \frac{2}{n_r - 1} \Upsilon_{iil} + \Upsilon_{ijl} + \Upsilon_{jil} &\prec 0, \quad i, j, l \in \mathcal{I}_{n_r}, \quad i \neq j. \end{aligned}$$

Lemma 2 ([37]). Given matrices \mathcal{B} and \mathcal{Y} , there exists a matrix \mathcal{X} such that $\mathcal{X}\mathcal{B} = \mathcal{Y}$ if and only if $\mathcal{Y}\mathcal{B}^\dagger\mathcal{B} = \mathcal{X}$. Moreover, the general solution to $\mathcal{X}\mathcal{B} = \mathcal{Y}$ is given by $\mathcal{X} = \mathcal{Y}\mathcal{B}^\dagger + \mathcal{S}(I - \mathcal{B}\mathcal{B}^\dagger)$, where \mathcal{S} is an arbitrary matrix of appropriate dimension.

B. LMI-Based UIO Design for Uncertain LPV Systems

The following theorem provides sufficient conditions to guarantee that system (18) is globally uniformly ℓ_∞ -stable.

Theorem 1. If there exist matrices $S \in \mathbb{R}^{n_x \times n_x}$ and $T \in \mathbb{R}^{n_x \times n_y}$ satisfying (16), positive definite matrices $P_i \in \mathbb{R}^{n_x \times n_x}$, matrices $G_i \in \mathbb{R}^{n_x \times n_x}$ and $L_i \in \mathbb{R}^{n_x \times n_y}$, for $i \in \mathcal{I}_{n_r}$, positive scalars $\alpha \leq 1$, μ and ν , such that the following optimization problem is achievable:

$$\text{minimize } \nu + \mu \quad (24)$$

subject to

$$\Xi_{iil} \succ 0 \quad (25)$$

$$\frac{2}{n_r - 1} \Xi_{iil} + \Xi_{ijl} + \Xi_{jil} \succ 0 \quad (26)$$

$$\begin{bmatrix} P_i & \star & \star & \star \\ 0 & \mu I & \star & \star \\ I & 0 & I & \star \\ (CD)^\dagger CA_i & (CD)^\dagger CE & 0 & I \end{bmatrix} \succeq 0 \quad (27)$$

for $i, j, l \in \mathcal{I}_{n_r}$ and $i \neq j$, with

$$\Xi_{ijl} = \begin{bmatrix} (1 - \alpha)P_i & \star & \star \\ 0 & \alpha\nu I & \star \\ G_i SA_j - L_i C & G_i SE & G_i + G_i^\top - P_l \end{bmatrix}.$$

Then, the estimation error dynamics (18) is globally uniformly ℓ_∞ -stable with an optimized performance level $\gamma = \sqrt{\nu + \mu}$.

Proof. Using Lemma 1 and the convex sum property (12) of the membership functions, it follows from (25) and (26) that

$$\begin{bmatrix} (1 - \alpha)P(\mathbf{h}) & \star & \star \\ 0 & \alpha\nu I & \star \\ G(\mathbf{h})SA(\mathbf{h}) - L(\mathbf{h})C & G(\mathbf{h})SE & \Pi(\mathbf{h}, \mathbf{h}_+) \end{bmatrix} \succ 0 \quad (28)$$

with

$$\begin{aligned} \Pi(\mathbf{h}, \mathbf{h}_+) &= G(\mathbf{h}) + G(\mathbf{h})^\top - P(\mathbf{h}_+) \\ P(\mathbf{h}) &= \sum_{i=1}^{n_r} h_i(\boldsymbol{\theta}_k) P_i, \quad P(\mathbf{h}_+) = \sum_{i=1}^{n_r} h_i(\boldsymbol{\theta}_{k+1}) P_i. \end{aligned}$$

Note that condition (28) implies that $P(\mathbf{h}) \succ 0$, and

$$\Pi(\mathbf{h}, \mathbf{h}_+) = G(\mathbf{h}) + G(\mathbf{h})^\top - P(\mathbf{h}_+) \succ 0 \quad (29)$$

for $\forall \mathbf{h}, \mathbf{h}_+ \in \mathcal{H}$. Since $\Pi(\mathbf{h}, \mathbf{h}_+) \succ 0$, it follows from (29) that $G(\mathbf{h}) + G(\mathbf{h})^\top \succ 0$. This, in turn, ensures the existence of the matrix inversion $G(\mathbf{h})^{-1}$. We multiply the matrix inequality (28) with

$$\begin{bmatrix} I & 0 & -\mathcal{A}^\top(\mathbf{h}) \\ 0 & I & -E^\top S^\top \end{bmatrix}$$

on the left and its transpose on the right, it follows that

$$\begin{bmatrix} \mathcal{A}^\top(\mathbf{h}) \\ E^\top S^\top \end{bmatrix} P(\mathbf{h}_+) \begin{bmatrix} \mathcal{A}(\mathbf{h}) & SE \end{bmatrix} - \mathcal{P}(\mathbf{h}) \prec 0 \quad (30)$$

with

$$\mathcal{P}(\mathbf{h}) = \begin{bmatrix} (1 - \alpha)P(\mathbf{h}) & 0 \\ 0 & \alpha\nu I \end{bmatrix}.$$

Pre- and post-multiplying (30) with $[e_k^\top \ w_k^\top]^\top$ and its transpose, we can obtain the following inequality after some algebraic manipulations:

$$\Delta\mathcal{V}(e_k) + \alpha(\mathcal{V}(e_k) - \nu w_k^\top w_k) < 0 \quad (31)$$

where the parameter-dependent Lyapunov function candidate $\mathcal{V}(e_k)$ is used for stability analysis, defined as

$$\mathcal{V}(e_k) = e_k^\top P(\mathbf{h})e_k. \quad (32)$$

The variation $\Delta\mathcal{V}(e_k)$ of the Lyapunov function candidate (32) along the trajectory of the error dynamics (18) is given by

$$\begin{aligned} \Delta\mathcal{V}(e_k) &= \mathcal{V}(e_{k+1}) - \mathcal{V}(e_k) \\ &= e_{k+1}^\top P(\mathbf{h}_+)e_{k+1} - e_k^\top P(\mathbf{h})e_k. \end{aligned} \quad (33)$$

We distinguish the two following cases.

Case 1. If $w_k = 0$, for $\forall k \in \mathbb{N}$, then it follows from (31) that

$$\Delta\mathcal{V}(e_k) + \alpha\mathcal{V}(e_k) < 0, \quad \forall k \in \mathbb{N} \quad (34)$$

where $\Delta\mathcal{V}(e_k)$ is given in (33). Condition (34) proves Property (P1) on the exponential stability with a decay rate α of the estimation error system (18).

Case 2. If $w_k \neq 0$ and $\{w_k\}_{k \in \mathbb{N}} \in \ell_\infty$, then it follows from (31) that

$$\mathcal{V}(e_k) < (1 - \alpha)\mathcal{V}(e_{k-1}) + \alpha\nu \|w_{k-1}\|^2, \quad \forall k \geq 1. \quad (35)$$

By recursivity and since $\alpha \in (0, 1)$, it follows from (35) that

$$\begin{aligned} \mathcal{V}(e_k) &< (1 - \alpha)^k \mathcal{V}(e_0) + \alpha\nu \sum_{i=0}^{k-1} (1 - \alpha)^i \|w_{k-1-i}\|^2 \\ &< (1 - \alpha)^k \mathcal{V}(e_0) + \alpha\nu \|w\|_{\ell_\infty}^2 \sum_{i=0}^{k-1} (1 - \alpha)^i \\ &< (1 - \alpha)^k \mathcal{V}(e_0) + \nu \|w\|_{\ell_\infty}^2, \quad \forall k \geq 1 \end{aligned} \quad (36)$$

which guarantees that e_k is uniformly bounded for any initial condition e_0 and any sequence $\{w_k\}_{k \in \mathbb{N}} \in \ell_\infty$.

Since $\mathbf{h} \in \mathcal{H}$, multiplying inequality (27) with $h_i(\theta_k)$, for $i \in \mathcal{I}_{n_r}$, and summing up, it follows that

$$\begin{bmatrix} P(\mathbf{h}) & \star & \star & \star \\ 0 & \mu I & \star & \star \\ I & 0 & I & \star \\ (CD)^\dagger CA(\mathbf{h}) & (CD)^\dagger CE & 0 & I \end{bmatrix} \succeq 0. \quad (37)$$

Applying the Schur complement lemma [27], we can show that inequality (37) is equivalent to

$$\begin{bmatrix} P(\mathbf{h}) & \star \\ 0 & \mu I \end{bmatrix} - \mathcal{E}(\mathbf{h})^\top \mathcal{E}(\mathbf{h}) \succeq 0. \quad (38)$$

where $\mathcal{E}(\mathbf{h})$ is defined in (21). Pre- and post-multiplying (38) with $[e_k^\top \ w_k^\top]^\top$ and its transpose while taking into account the definition of z_k in (20), the following inequality can be obtained after some simple manipulations:

$$\|z_k\|^2 \leq \mathcal{V}(e_k) + \mu \|w_k\|^2. \quad (39)$$

It follows from (36) and (39) that

$$\|z_k\| \leq \sqrt{\mathcal{V}(e_0)}(1 - \alpha)^{k/2} + \gamma \|w\|_{\ell_\infty}, \quad \forall k \geq 1 \quad (40)$$

with $\gamma = \sqrt{\nu + \mu}$. For any initial condition e_0 , it follows from (40) that

$$\limsup_{k \rightarrow \infty} \|z_k\| \leq \gamma \|w\|_{\ell_\infty}. \quad (41)$$

Conditions (36), (40) and (41) ensure Property (P2). Moreover, minimizing $\nu + \mu$ in (24) leads to a minimization of γ , *i.e.*, an optimized estimation performance under the disturbance effect w_k . This concludes the proof. \square

Note that the sufficient conditions in Theorem 1 are expressed in terms of nonconvex matrix inequalities, which cannot be directly applied for UIO design. To derive a set of solvable LMI-based design conditions, we reformulate condition (16) as

$$\begin{bmatrix} S & T \end{bmatrix} \begin{bmatrix} I & D \\ C & 0 \end{bmatrix} = \begin{bmatrix} I & 0 \end{bmatrix}. \quad (42)$$

Since the rank condition (13) holds, a solution for the matrix equation (42) exists. Applying Lemma 2 with

$$\mathcal{X} = \begin{bmatrix} S & T \end{bmatrix}, \quad \mathcal{B} = \begin{bmatrix} I & D \\ C & 0 \end{bmatrix}, \quad \mathcal{Y} = \begin{bmatrix} I & 0 \end{bmatrix}$$

the following solution for S and T can be obtained:

$$\begin{bmatrix} S & T \end{bmatrix} = \begin{bmatrix} I & 0 \end{bmatrix} \begin{bmatrix} I & D \\ C & 0 \end{bmatrix}^\dagger + \mathcal{S} \left(I - \begin{bmatrix} I & D \\ C & 0 \end{bmatrix} \begin{bmatrix} I & D \\ C & 0 \end{bmatrix}^\dagger \right) \quad (43)$$

where \mathcal{S} is an arbitrary matrix of appropriate dimension. Then, the proposed UIO design for LPV systems is summarized in Algorithm 1.

Algorithm 1 UIO Design with ℓ_∞ -Gain Performance

- 1: **Inputs:** LPV uncertain system (11)
 - 2: **Outputs:** Observer (14) such that system (18) is globally uniformly ℓ_∞ -stable
 - 3: **if condition (13) verified then**
 - 4: proceed the UIO design
 - 5: **else**
 - 6: unable to design UIO with the proposed method
 - 7: **end if**
 - 8: Compute matrices S and T with (43)
 - 9: Solve LMI-based optimization problem (24)
 - 10: Get G_i and L_i , for $i \in \mathcal{I}_{n_r}$
 - 11: Construct $G(\mathbf{h})$ and $L(\mathbf{h})$ with (15)
 - 12: Construct LPV observer (14)
-

Remark 5. The UIO design procedure in Algorithm 1 is reformulated as a convex optimization problem under LMI constraints, which can be effectively solved with YALMIP toolbox and SPDT3 solver [38].

Remark 6. For UI estimation, the future information of the measured output y_{k+1} is required in (14). It is emphasized that this UI estimation expression is only used for theoretical analysis. In practice, the UI estimation is implemented as

$$\hat{\mathbf{d}}_{k-1} = (CD)^\dagger (y_k - CA(\mathbf{h}_-) \hat{\mathbf{x}}_{k-1} - CBu_{k-1}). \quad (44)$$

with $\mathbf{h}_- = [h_1(\theta_{k-1}), h_2(\theta_{k-1}), \dots, h_{n_r}(\theta_{k-1})]^\top$. Since the past values of all signals involved in (44) are available, it is

always possible to estimate the one-step-back UI value \hat{d}_{k-1} . This practical solution is frequently used in UI estimation with decoupling-based approaches [11], [34]. Note also from (44) that directly using y_k to compute \hat{d}_k can make the UI estimation performance of the proposed decoupling-based method more sensitive to measurement noises/disturbances compared to the estimation results obtained from PI observers.

V. ILLUSTRATIVE RESULTS AND DISCUSSIONS

This section presents HiL results with suitable comparative studies to show the effectiveness of the proposed UIO with respect to related literature. All the test scenarios are performed with a human driver and the SHERPA interactive driving simulator, shown in Fig. 4. The SensoDrive force feedback steering wheel can provide the real-time information about the driver steering torque. Moreover, the SHERPA simulator is fully instrumented to measure all vehicle state variables. Within the SCANer™ Studio 1.6 environment, the proposed UIO is implemented in the SHERPA simulator through the Matlab/Simulink software. A demonstration video of the SHERPA simulator is available at <https://shorturl.at/eloQY>.



Fig. 4. SHERPA simulator (left) and its steering system (right).

Following the UIO design procedure in Algorithm 1, we can obtain an UIO solution for HiL validations with $\alpha = 0.01$ and $\gamma_{\min} = 3.94$. For brevity, only some of the decision matrices obtained with Theorem 1 are given by

$$L_1 = \begin{bmatrix} -9232.74 & 47014.28 & 1294.44 \\ 182326.84 & 160138.57 & 562.18 \\ 9402.23 & 4436867.44 & 42033.74 \\ 237.12 & 808.77 & -50.80 \end{bmatrix}$$

$$G_1 = \begin{bmatrix} 15320.49 & -2846.85 & -40000.68 & -1008.81 \\ * & 580995.48 & -47481.23 & -1197.47 \\ * & * & 9295855.94 & 12263.39 \\ * & * & * & 8809906.99 \end{bmatrix}$$

$$P_1 = \begin{bmatrix} 11658.67 & 7453.41 & -57439.03 & -1448.61 \\ * & 361250.98 & -76039.53 & -1917.69 \\ * & * & 10338093.63 & 23129.95 \\ * & * & * & 9421546.56 \end{bmatrix}$$

$$S = \begin{bmatrix} 1.00 & 0 & 0 & 0 \\ * & 0.50 & 0 & 0 \\ * & * & 0.50 & 0 \\ * & * & * & 0 \end{bmatrix}, \quad T = \begin{bmatrix} 0 & 0 & 0 \\ 0.50 & 0 & 0 \\ 0 & 0.50 & 0 \\ 0 & 0 & 1.00 \end{bmatrix}.$$

The following four test scenarios are selected to verify the practical estimation performance of the proposed UIO under different driving conditions.

A. Scenario 1: Manual Driving with Zigzag Steering Pattern

For this test scenario, the driver performs a manual driving task without automation assistance, *i.e.*, $T_a = 0$, at a constant vehicle speed $v_x = 22$ [m/s]. The corresponding vehicle trajectory is shown in Fig. 5(a). The driver deliberately executes a zigzag steering pattern during this test to provoke the uncertain EPS dynamics, as represented by the high-frequency behaviors of the steering angle and the steering rate in Figs. 5(b) and (c). The estimation results of the unmeasured vehicle lateral speed v_y and the unknown driver steering torque T_d are depicted in Figs. 6(a) and (b), respectively. We can see that the proposed UIO can achieve an accurate estimation performance despite the high-frequency nature of the measured signals and the small amplitude of the driver torque T_d .

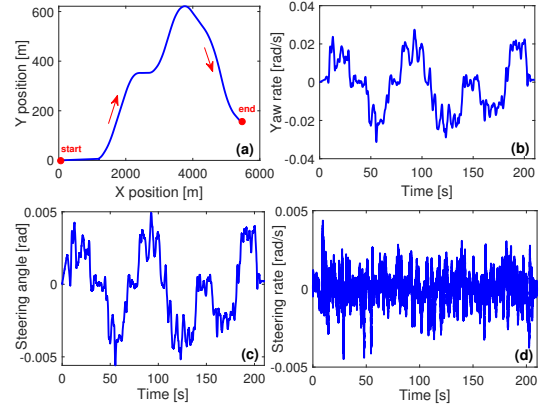


Fig. 5. Scenario 1. (a) Vehicle trajectory, (b) Yaw rate, (c) Steering angle, (d) Steering rate.

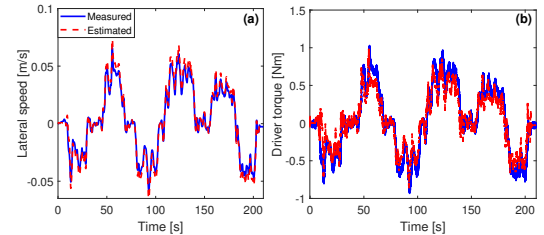


Fig. 6. Estimation performance obtained with Scenario 1. (a) Lateral speed, (b) Driver torque.

To provide a quantitative performance analysis, Table II summarizes the error indices obtained with the proposed LPV observer. Note that E_{mean} is the average error, E_{max} is the maximal error, RMS [%] is the root-mean-square error, and GoF [%] is the goodness of fit between the estimated and the measured signals. We can see that the excellent estimation performance is numerically confirmed by the small error indicators and a high goodness of fit level.

TABLE II
NUMERICAL STATISTICS ON ESTIMATION ERRORS FOR SCENARIO 1.

Error index	E_{mean}	E_{max}	RMS	GoF
T_d [Nm]	0.104	0.607	9.057	80.060
v_y [m/s]	0.003	0.013	4.828	86.179

B. Scenario 2: Cooperative Driving on a Real Test Track

This test is performed under smooth driving conditions on the Satory test track, which is approximately 2.3 km long, with various levels of road curvature, depicted in Fig. 7(a). The human driver cooperatively executes the lane-keeping task with the assistance system and maintains a time-varying longitudinal speed, as shown in Figs. 7(b) and (c). As depicted in Fig. 8, despite significant variations in the vehicle speed v_x , the assistance torque T_a , and the driver steering torque T_d , the proposed UIO accurately reconstructs the unmeasured signals v_y and T_d throughout the entire cooperative driving task. This is further numerically confirmed by the small error indices summarized in Table III.

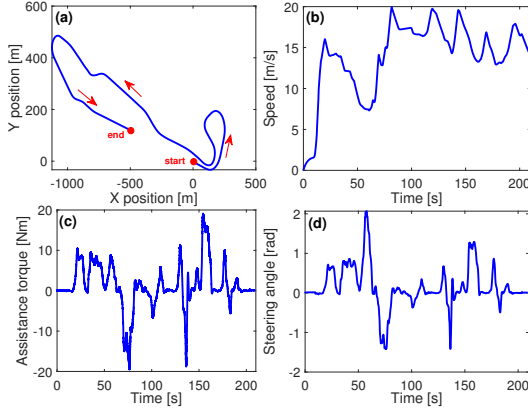


Fig. 7. Scenario 2. (a) Vehicle trajectory, (b) Vehicle speed, (c) Assistance torque, (d) Steering angle.

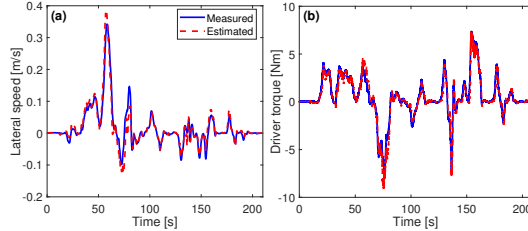


Fig. 8. Estimation performance obtained with Scenario 2. (a) Lateral speed, (b) Driver torque.

TABLE III

NUMERICAL STATISTICS ON ESTIMATION ERRORS FOR SCENARIO 1.

Error index	E_{mean}	E_{max}	RMS	GoF
T_d [Nm]	0.432	4.024	6.013	76.845
v_y [m/s]	0.008	0.094	2.410	82.334

C. Scenario 3: Driving with Automation-Driver Conflict

For this scenario, we consider a driving task in a driver-automation conflict situation, where the vehicle runs at a constant speed of $v_x = 25$ [m/s] on the trajectory depicted in Fig. 9(a). The conflict situation is characterized by the fact that the driver and the assistance torques are in opposite sign during almost the whole test as shown in Fig. 9(b). This induces a

high vehicle dynamics solicitation as presented by the yaw rate and steering angle signals in Figs. 9(c) and (d), respectively. Fig. 10 shows that despite this challenging scenario, the lateral speed v_y and the driver steering torque T_d are very well estimated with the proposed UIO, which is also confirmed by the performance indicators in Table IV.

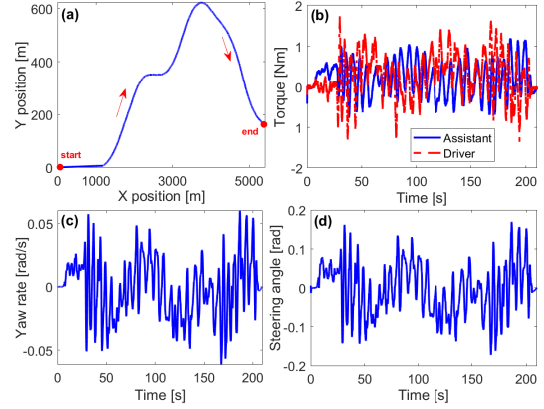


Fig. 9. Scenario 3. (a) Vehicle trajectory, (b) Assistance and driver torques, (c) Yaw rate, (d) Steering angle.

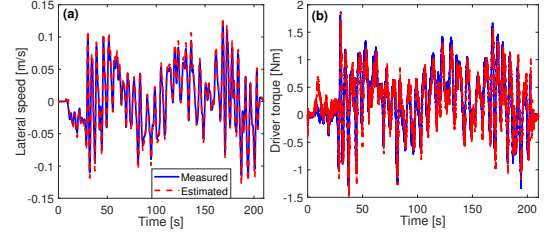


Fig. 10. Estimation performance obtained with Scenario 3. (a) Lateral speed, (b) Driver torque.

TABLE IV

NUMERICAL STATISTICS ON ESTIMATION ERRORS FOR SCENARIO 3.

Error index	E_{mean}	E_{max}	RMS	GoF
T_d [Nm]	0.259	1.497	7.560	86.644
v_y [m/s]	0.005	0.015	3.814	87.782

D. Scenario 4: Estimation Performance Comparison

This test is used for comparison purposes with the LPV observer proposed in [21], which can already provide a better estimation performance than the PMI observer in [25]. The driving is composed of two phases: autonomous mode from 0s to 33s, and driver-automation shared control mode from 33s to 60s, as shown in Figs. 11(a) and (b). Note also that during the second driving phase, the human driver has to perform three unexpected obstacle avoidance maneuvers around 35s, 39s and 55s to purposely create some driver-automation conflicting situations. To emphasize the practical interest of the proposed method, we consider the case where F_f and F_r represent 30% of modeling uncertainties in the lateral tires forces. It can be seen in Fig. 12(a) that both

observers provide a similar estimation performance for v_y when driving on the straight road section, *i.e.*, the second driving phase. However, during the tight curves, *i.e.*, the first driving phase, the estimation quality of the LPV observer [21] is degraded, which is not the case of the new estimation method. Fig. 12(b) shows that the proposed UIO can prevent some usual peaks in the estimation of the driver torque T_d , especially when T_d becomes large to counteract the effect of T_a as during driver-automation conflicting situations. The numerical comparison results given in Table V clearly confirm the outperformance of the proposed method with respect to the existing LPV observer [21].

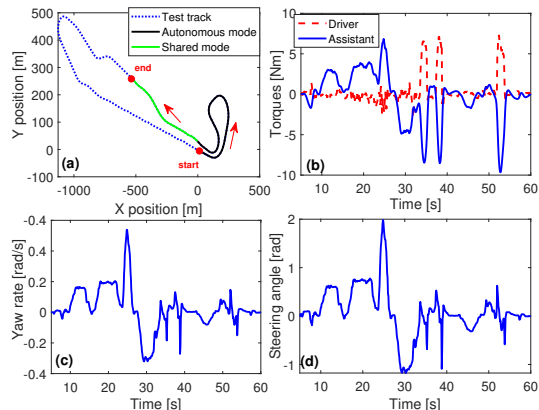


Fig. 11. Scenario 4. (a) Vehicle trajectory, (b) Assistance and driver torques, (c) Yaw rate, (d) Steering angle.

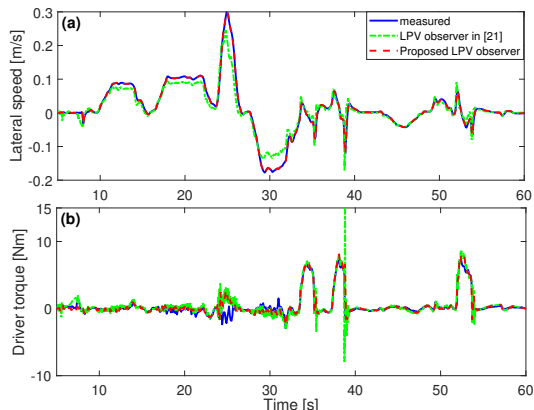


Fig. 12. Estimation performance comparison between the proposed observer and the LPV observer in [21] obtained with Scenario 4. (a) Lateral speed, (b) Driver torque.

VI. CONCLUSIONS AND FUTURE WORKS

A parameter-dependent UIO-based method has been proposed to jointly estimate the sideslip angle and the unknown driver steering torque for IVs within the human-machine shared driving framework. To deal with the time-varying nature of the vehicle speed involved in the vehicle dynamics, we represent the vehicle system as a polytopic LPV model. An LPV vertex reduction is performed to reduce the design conservatism and numerical complexity while avoiding approximation errors. Using an UI decoupling technique, the influence

TABLE V
ESTIMATION PERFORMANCE COMPARISON.

Error index	Proposed observer	LPV observer [21]
$E_{\text{mean}} T_d$	0.039	0.325
$E_{\text{mean}} v_y$	0.004	0.009
$E_{\text{max}} T_d$	1.686	4.807
$E_{\text{max}} v_y$	0.062	0.144
RMS T_d	3.284	11.437
RMS v_y	2.334	4.874
GoF T_d	82.736	67.605
GoF v_y	95.744	81.181

of the unknown driver steering torque is decoupled from the estimation error dynamics. This latter only depends on the unknown exogenous disturbances, issued from the modeling uncertainties of lateral tires forces and EPS dynamics. Via Lyapunov stability theory, the UIO design is reformulated as a convex optimization problem under LMI constraints, where the estimation errors of the sideslip angle and the driver torque can be set arbitrarily small via an optimized ℓ_∞ -gain performance. HiL results obtained with the SHERPA interactive driving simulator and a human driver have been presented to show the effectiveness of the new UIO-based estimation method. For future works, the proposed UIO structure will be incorporated into a hierarchical human-machine shared control architecture. Special emphasis are placed on addressing actuator faults and/or driver failures. User-test experiments with several driver participants are also necessary to evaluate the practical performance of the proposed UIO-based shared control solution.

REFERENCES

- [1] C. Huang, L. Li, Y. Liu, and L. Xiao, "Robust observer based intermittent forces estimation for driver intervention identification," *IEEE Trans. Veh. Technol.*, vol. 69, no. 4, pp. 3628–3640, 2020.
- [2] P. Li, A.-T. Nguyen, H. Du, Y. Wang, and H. Zhang, "Polytopic LPV approaches for intelligent automotive systems: State of the art and future challenges," *Mech. Syst. Signal Process.*, vol. 161, p. 107931, 2021.
- [3] Z. Xue, S. Cheng, L. Li, Z. Zhong, and H. Mu, "A robust unscented M-estimation-based filter for vehicle state estimation with unknown input," *IEEE Trans. Veh. Technol.*, vol. 71, no. 6, pp. 6119–6130, 2022.
- [4] A.-T. Nguyen, C. Sentouh, and J.-C. Popieul, "Driver-automation cooperative approach for shared steering control under multiple system constraints: Design and experiments," *IEEE Trans. Indus. Electron.*, vol. 64, no. 5, pp. 3819–3830, 2017.
- [5] P. Hang, X. Chen, and W. Wang, "Cooperative control framework for human driver and active rear steering system to advance active safety," *IEEE Trans. Intell. Veh.*, vol. 6, no. 3, pp. 460–469, 2021.
- [6] A. Arab, K. Yu, J. Yu, and J. Yi, "Motion planning and control of autonomous aggressive vehicle maneuvers," *IEEE Trans. Autom. Sci. Eng.*, pp. 1–13, 2023.
- [7] C. Sentouh, A.-T. Nguyen, M. Benloucif, and J.-C. Popieul, "Driver-automation cooperation oriented approach for shared control of lane keeping assist systems," *IEEE Trans. Control Syst. Technol.*, vol. 27, no. 5, pp. 1962–1978, 2019.
- [8] J. Han, J. Zhao, B. Zhu, and D. Song, "Adaptive steering torque coupling framework considering conflict resolution for human-machine shared driving," *IEEE Trans. Intell. Transp. Syst.*, vol. 23, no. 8, pp. 10983–10995, 2021.
- [9] J. Liu, Q. Dai, H. Guo, J. Guo, and H. Chen, "Human-oriented online driving authority optimization for driver-automation shared steering control," *IEEE Trans. Intell. Veh.*, vol. 7, no. 4, pp. 863–872, 2022.
- [10] B. Zhang, H. Du, J. Lam, N. Zhang, and W. Li, "A novel observer design for simultaneous estimation of vehicle steering angle and sideslip angle," *IEEE Trans. Indus. Electron.*, vol. 63, no. 7, pp. 4357–4366, 2016.

- [11] A.-T. Nguyen, T. Dinh, T.-M. Guerra, and J. Pan, "Takagi-Sugeno fuzzy unknown input observers to estimate nonlinear dynamics of autonomous ground vehicles: Theory and real-time verification," *IEEE/ASME Trans. Mechatron.*, vol. 26, no. 3, pp. 1328–1338, 2021.
- [12] X. Wang, L. Guo, and Y. Jia, "Online sensing of human steering intervention torque for autonomous driving actuation systems," *IEEE Sens. J.*, vol. 18, no. 8, pp. 3444–3453, 2018.
- [13] J. Wu, J. Zhang, Y. Tian, and L. Li, "A novel adaptive steering torque control approach for human-machine cooperation autonomous vehicles," *IEEE Trans. Transp. Electrifi.*, vol. 7, no. 4, pp. 2516–2529, 2021.
- [14] X. Zhou, Z. Wang, H. Shen, and J. Wang, "A mixed $\mathcal{L}_1/\mathcal{H}_2$ robust observer with an application to driver steering torque estimation for autopilot-human shared steering," *J. Dyn. Sys., Meas., Control.*, vol. 144, no. 7, p. 071007, 2022.
- [15] W. Schinkel, T. van der Sande, and H. Nijmeijer, "Driver intervention detection via real-time transfer function estimation," *IEEE Trans. Intell. Transp. Syst.*, vol. 22, no. 2, pp. 772–781, 2021.
- [16] Q. Li, Z. Wang, W. Wang, C. Zeng, C. Wu, G. Li, J.-S. Heh, and B. Cheng, "A human-centered comprehensive measure of take-over performance based on multiple objective metrics," *IEEE Trans. Intell. Transp. Syst.*, vol. 24, no. 4, pp. 4235–4250, 2023.
- [17] C. Huang, C. Lv, P. Hang, Z. Hu, and Y. Xing, "Human-machine adaptive shared control for safe driving under automation degradation," *IEEE Intell. Transp. Syst. Mag.*, vol. 14, no. 2, pp. 53–66, 2022.
- [18] S. Muhlbacher-Karrer, A. H. Mosa, L.-M. Faller, M. Ali, R. Hamid, H. Zangl, and K. Kyamakya, "A driver state detection system—combining a capacitive hand detection sensor with physiological sensors," *IEEE Trans. Instrum. Meas.*, vol. 66, no. 4, pp. 624–636, 2017.
- [19] B.-G. Lee and W.-Y. Chung, "Wearable glove-type driver stress detection using a motion sensor," *IEEE Trans. Intell. Transp. Syst.*, vol. 18, no. 7, pp. 1835–1844, 2017.
- [20] G. Li, W. Yan, S. Li, X. Qu, W. Chu, and D. Cao, "A temporal-spatial deep learning approach for driver distraction detection based on EEG signals," *IEEE Trans. Autom. Sci. Eng.*, vol. 19, no. 4, pp. 65–77, 2022.
- [21] A.-T. Nguyen, T.-M. Guerra, C. Sentouh, and H. Zhang, "Unknown input observers for simultaneous estimation of vehicle dynamics and driver torque: Theoretical design and hardware experiments," *IEEE/ASME Trans. Mechatron.*, vol. 24, no. 6, pp. 2508–2518, 2019.
- [22] S. Kaplan, M. A. Guvensan, A. G. Yavuz, and Y. Karalurt, "Driver behavior analysis for safe driving: A survey," *IEEE Trans. Intell. Transp. Syst.*, vol. 16, no. 6, pp. 3017–3032, 2015.
- [23] S. You, G. Kim, S. Lee, D. Shin, and W. Kim, "Neural approximation-based adaptive control using reinforced gain for steering wheel torque tracking of electric power steering system," *IEEE Trans. Syst., Man, Cybern.: Syst.*, vol. 53, no. 7, pp. 4216–4225, 2023.
- [24] K. Yamamoto, O. Sename, D. Koenig, and P. Moulaire, "Design and experimentation of an LPV extended state feedback control on EPS systems," *Control Eng. Pract.*, vol. 90, pp. 123–132, 2019.
- [25] B. Soualmi, C. Sentouh, and J.-C. Popieul, "Both vehicle state and driver's torque estimation using unknown input proportional multi-integral T-S observer," in *Europ. Control Conf.*, 2014, pp. 2957–2962.
- [26] J. Pan, A.-T. Nguyen, T.-M. Guerra, and D. Ichalal, "A unified framework for asymptotic observer design of fuzzy systems with unmeasurable premise variables," *IEEE Trans. Fuzzy Syst.*, vol. 29, no. 10, pp. 2938–2948, 2021.
- [27] S. Boyd, L. El Ghaoui, E. Feron, and V. Balakrishnan, *Linear Matrix Inequalities in System and Control Theory*. Philadelphia, PA: SIAM, 1994, vol. 15.
- [28] A.-T. Nguyen, C. Sentouh, and J.-C. Popieul, "Fuzzy steering control for autonomous vehicles under actuator saturation: Design and experiments," *J. Franklin Inst.*, vol. 355, no. 18, pp. 9374–9395, 2018.
- [29] R. Rajamani, *Vehicle Dynamics and Control*. Springer US, 2012.
- [30] N. Enache, M. Netto, S. Mammam, and B. Lusetti, "Driver steering assistance for lane departure avoidance," *Control Eng. Pract.*, vol. 17, no. 6, pp. 642–651, 2009.
- [31] E. Ono, S. Hosoe, H. Tuan, and S. Doi, "Bifurcation in vehicle dynamics and robust front wheel steering control," *IEEE Trans. Control Syst. Technol.*, vol. 6, no. 3, pp. 412–420, 1998.
- [32] X. Chen, S. Li, L. Li, W. Zhao, and S. Cheng, "Longitudinal-lateral-cooperative estimation algorithm for vehicle dynamics states based on adaptive-square-root-cubature-Kalman-filter and similarity-principle," *Mech. Syst. Signal Process.*, vol. 176, p. 109162, 2022.
- [33] Q. Jia, W. Chen, Y. Zhang, and H. Li, "Fault reconstruction and fault-tolerant control via learning observers in Takagi-Sugeno fuzzy descriptor systems with time delays," *IEEE Trans. Indus. Electron.*, vol. 62, no. 6, pp. 3885–3895, 2015.
- [34] H. Trinh and T. Fernando, *Functional Observers for Dynamical Systems*. Springer Science & Business Media, 2011, vol. 420.
- [35] S. Zak, *Systems and Control*. New York: Oxford University Press, 2003, vol. 198.
- [36] H.-D. Tuan, P. Apkarian, T. Narikiyo, and Y. Yamamoto, "Parameterized linear matrix inequality techniques in fuzzy control system design," *IEEE Trans. Fuzzy Syst.*, vol. 9, no. 2, pp. 324–332, 2001.
- [37] A. Laub, *Matrix Analysis for Scientists and Engineers*. Philadelphia, PA, USA: SIAM, 2005, vol. 91.
- [38] J. Löfberg, "Yalmip: A toolbox for modeling and optimization in Matlab," in *IEEE Int. Symp. Comput. Aided Control Syst. Des.*, Taipei, Sept. 2004, pp. 284–289.



Anh-Tu Nguyen (M'18, SM'21) is an Associate Professor at the INSA Hauts-de-France, Université Polytechnique Hauts-de-France, Valenciennes, France. He received the degree in engineering and the M.Sc. degree in automatic control from Grenoble Institute of Technology, France, in 2009, and the Ph.D. degree in automatic control from the University of Valenciennes, France, in 2013. He is an Associate Editor for several journals such as *IEEE/ASME TMECH*, *IEEE T-ITS*, *IFAC CEP*, *ISA Transactions*. His research interests include robust control and estimation, human-in-the-loop control, and mechatronic applications.



Thierry-Marie Guerra received the Ph.D. degree in automatic control in 1991 from University of Valenciennes, France. He is a Full Professor with the Polytechnic University Hauts-de-France, France. His research fields are Takagi-Sugeno control and observation, LMI constraints and applications to mobility, soft robotics, and disabled persons. Prof. Guerra is the chair of the IFAC Technical Committee 3.2 "Computational Intelligence in Control", an Associate Editor of *FSS* and *IEEE TFS*.



Chouki Sentouh received the PhD degree in automatic control from the University of Evry, France, in 2007. He is an Associate Professor at the Université Polytechnique Hauts-de-France, laboratory LAMIH UMR CNRS 8201, France. His research fields include robust control and observation applied to automotive control, driver assistance systems, human driver modeling and cooperation in intelligent transportation systems.



Jean-Christophe Popieul received the Ph.D. degree in automatic control in 1994 from University of Valenciennes, France. He is Professor at the Université Polytechnique Hauts-de-France, laboratory LAMIH UMR CNRS 8201, France. Specialized in human-centered automation, he participated in many collaborative projects dealing with ADASs. He is currently working on control sharing for driving automation and is the coordinator of the RITMEA project with 350 researchers involved and several other national and international projects.